Minimization of wear in a transfer chute by geometric optimization of convex pattern surface: A DEM study

Yunpeng Yan[1], Wouter Vreeburg[1], Guangming Chen[2] and Dingena Schott[1]

[1] Department of Maritime and Transport Technology, Delft University of Technology, Delft, The Netherlands
2628 CD Delft
Y.Yan1@tudelft.nl

[2] College of Mechanical and Electrical Engineering, Nanjing University of Aeronautics and Astronautics, Nanjing, China
210016
guangming2012@hotmail.com

Keywords transfer chute; material equipment interaction; wear reduction; optimization of bionic convexes; DEM; design of experiments

Abstract Using bionic surface on the material equipment interface of bulk handling equipment is a promising solution for wear reduction. A bionic surface is a flat surface outfitted with a pattern of convexes that disrupt the natural sliding flow of bulk material. Previous numerical work has shown a significant reduction of wear of bionic surfaces compared to a smooth surface.

The aim of this paper is to study the influence of bionic configurations on wear reduction. Four geometric parameters were introduced to define the shape and size of these convex patterns. The geometric convex patterns were evaluated with the aid of Discrete Element Method (DEM). The simulated material was iron ore with d_{50} of 10 mm sliding down a smooth chute transitioning into bionic surface of different geometric configurations. Hertz-Mindlin (no slip) model and Archard wear model were implemented to calculate the sliding wear volume. The experimental plan was based on a full factorial design, which varied the parameters of a_0, a_0:b_0, c_0 and d_0.

Simulation results show that different patterns of convexes have different influence on wear volumes and velocities of particles. The factors a_0 and d_0 of each pattern have significant influence on sliding wear, while there are insignificant interactions between geometric parameters. It is found that the existence of convex patterns makes the particles closest to the chute's surface have the tendency to slow down, causing the remainder of the particles to slide and roll over these bottom particles instead of sliding directly over the surface.

1 INTRODUCTION

The increasing global demand for iron ore is placing greater emphasis on the need for higher mining production capacity [1]. On account of the abrasive nature of iron ore, large-scale handling commonly causes high wear on the surfaces of handling equipment [2]. Several locations with heavy wear are found on silo walls and chute bottom [3]. Wear causes volume loss from the surfaces of handling equipment and consequently accelerates the damage of equipment. To save economic cost and reduce downtime, the surface wear of bulk solids handling equipment must be reduced.

Several methods are applied to reduce surface wear. Roberts [3] optimized the curvature of transfer chutes based on the predictions of particle flow trajectories. Chumber [4] utilized wear-resistant materials and linings to protect equipment surfaces. Hilgraf [5, 6] added assistant components to utilize self-wear mechanism by the transported bulk solids. Dietmar [7] supplied additional power to reduce the contact for between particulate solids and equipment surface. Recent work by Chen [2] introduced a new method based on bionic design and developed convex pattern on a chute surface in order to minimize the sliding wear that occurs when a bulk material slides over the surface.

Chen predicted wear on smooth and non-smooth chute surfaces by a numerical approach using DEM. The discrete element method (DEM) was initially developed by Cundall and Strack [8] to predict mechanics of rocks that were composed by spherical particles. A series of contact models are developed to simulate behaviour of bulk solids [9]. For non-cohesive materials, the Hertz-Mindlin no-slip contact model [10,11] and Linear-Spring-Dashpot (LSD) model [12] are used. In bulk solids handling, the Hertz-Mindlin no-slip contact model has been used to predict the abrasion and impact on the liner [13], lifter [14], and screen mesh [15]. Furthermore, this model is used to predict impact force on transfer plate [16], transfer chute [17] and pipe wall [18]. Besides, the Hertz-Mindlin with Archard Wear model extends the standard H-M model to give an estimation of wear depth for geometry surfaces [19]. It is used to calibrate a large scale abrasive wear of tipper bodies during unloading of granular material [20].

Based on research [2], a bionic method is used to reduce wear on transfer chute. In this paper, the influence of parameters of bionic elements on wear of transfer chute will be studied. Besides, the interactions between parameters will also be investigated.

2 METHODOLOGY

The selected method for the design of experiments is explained briefly and used to create a research plan. The experimental simulation setup is illustrated, including all the simulation settings.

2.1 Dimensions of bionic model

Four parameters were introduced to define the shape and dimensions of these convex patterns, as shown in

Figure 1, and four different geometries were created and listed in Table 1: Geometrical parameters used to vary bionic surfaces in simulations (Group 1-4).

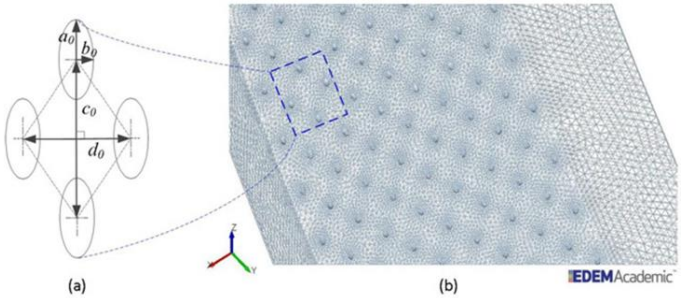

Figure 1: Parameters determining shape of bionic surface

Table 1: Geometrical parameters used to vary bionic surfaces in simulations

Geometrical parameters	Group 1	Group 2	Group 3	Group 4
Major radius a_0 (mm)	2	3	4	5
Minor radius b_0 (mm)	1.5	2	2.5	3
Vertical distance c_0 (mm)	30	40	50	60
Horizontal distance d_0 (mm)	25	30	35	40

2.1. Full factorial design approach

Design of experiments (DoE) is an optimization method which is a systematic method to determine the relationship between factors [21]. A DoE formulation called full factorial design (FFD) is chosen. FFD is suitable when more than three factors and interactions are considered [21-22]. This research applies 2-level FFD which works by choosing a high and low value for every factor.

The factors a_0, b_0, c_0 and d_0 are shown in Table 2, in which a ratio of a_0 : b_0 is used instead of b_0. This ratio is a representation of the eccentricity of the ellipsoid shape of the convexes and the height of the convexes is equal to the value of b_0. The high and low value are selected based on the geometric parameters in [2].

Table 2: The full factorial factors with corresponding high and low values

Factor	Low value (mm)	High value (mm)
a_0	2	6
a_0:b_0	1.3	1.7
c_0	25	50
d_0	25	50

An experimental plan is made which consists 17 simulations, including one reference simulation with smooth surface, as shown in Table 3.

Table 3:The simulation plan (0: smooth surface, 1-16: bionic surface)

Configuration	0	1	2	3	4	5	6	7	8	9	10	11	12	13	14	15	16
a_0 (mm)	-	2	6	2	6	2	6	2	6	2	6	2	6	2	6	2	6
a_0:b_0 (-)	-	1.3	1.3	1.7	1.7	1.3	1.3	1.7	1.7	1.3	1.3	1.7	1.7	1.3	1.3	1.7	1.7
c_0 (mm)	-	25	25	25	25	50	50	50	50	25	25	25	25	50	50	50	50
d_0 (mm)	-	25	25	25	25	25	25	25	25	25	50	50	50	50	50	50	50

2.2. Geometry creation

The shape of the geometry is shown in Figure 2. It allows the particles to slide from a smooth surface onto a bionic surface, as opposed to dropping the particles directly onto a bionic surface area.

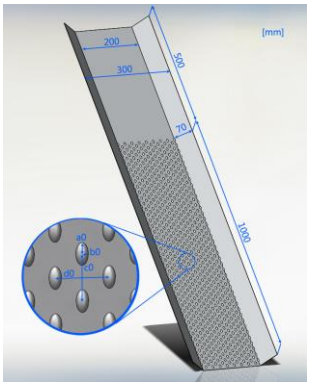

Figure 2: Chute geometry with dimensions

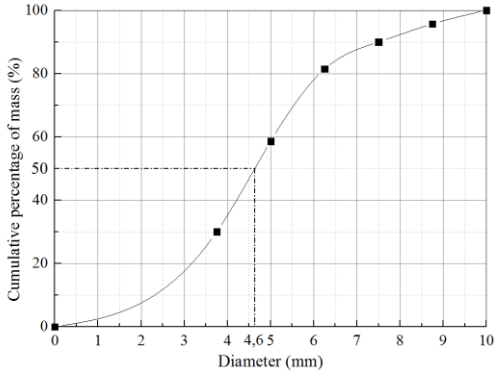

Figure 3: Particle size distribution

The particles are modelled as spheres with d_{50} of 4.6 mm and flow rate of 20 kg/s, and the particle size distribution is shown in Figure 3. The contact model and wear model are chosen as Herzt-Mindlin (no slip) and Archard wear model respectively. The simulation parameters are summarized in Table 3.

Table 3. Material properties and interactions

Parameters	Iron ore	Steel
Poisson's ratio (-)	0.24	0.3
Shear modulus (GPa)	65	78
Density (kg/m^3)	4865	7932
coefficient of restitution (-)	0.45	0.4
coefficient of static friction (-)	0.41	0.46
coefficient of rolling friction (-)	0.22	0.3

2.4 Index of evaluation

The sliding wear is measured on the part of the bionic surface with a steady flow of material. As can be seen in Figure 4 (left), a geometry bin is created over the bionic surface to measure the sliding wear. From a test run in Figure 4 (right), it can be seen that the material starts to pile up at the start of entering into bionic area. The middle circle in Figure 4 shows that the wear on the bionic surface is not steady yet and therefore the geometry bin is placed below this area. Simulation time is set as 1.2 seconds.

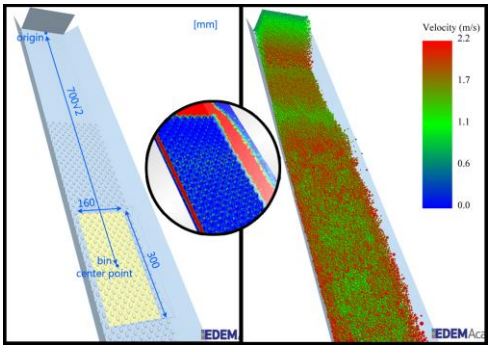

Figure 4: Position and dimensions of geometry bin for measuring sliding wear (left); Bulk flow over chute geometry showing build-up at start of bionic surface (right)

Since all the results approximate a linear increase in sliding wear, the gradient (slope) of each line is used to represent the wear per simulation.

3 RESULTS OF EXPERIMENTS

The results of the DoE are presented in this part. First the sliding wear results from the EDEM simulations are shown, which are then analysed through Minitab®17.

3.1 EDEM sliding wear results

Three repetitions of configuration 1 are performed to verify the simulation settings, as shown in Figure 5. The results are within a 98.8% confidence interval.

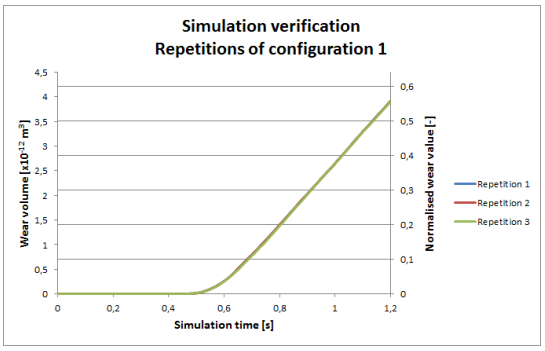

Figure 5: Graph with normalized sliding wear results of three repetitions (configuration 1)

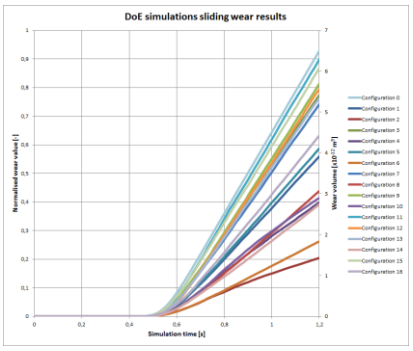

Figure 6: DoE simulations sliding wear results

Figure 6 shows the sliding wear results of the 17 simulations. It should be noted that the wear volume is normalized through divided by 7×10^{-9}. As can be seen in Figure 6, after around 0.5 seconds, the bulk flow reaches geometry bin and the wear is visible. After a slight curve upwards, all graphs follow an almost linear path. This suggests a steady flow of material passing the geometry bin. It is noted that configuration 0 shows the highest wear values. Configuration 11 and configuration 2 show the highest and lowest wear volumes in bionic configurations respectively.

The average of the slopes of every time interval (0.01s) between 1 second and 1.2 seconds is taken to get one value for the slope of every line. Comparing average values to all the slope values per time interval, they all fall within a 95% confidence interval, making it a valid method for obtaining a gradient value. The normalised wear results are presented in Table 4.

Table 4: Wear results of DoE simulations

Configu-ration	Normalised wear gradient	Configu-ration	Normalised wear gradient	Configu-ration	Normalised wear gradient	Configu-ration	Normalised wear gradient
0	1.42	4	0.59	8	0.73	12	1.29
1	0.90	5	0.94	9	1.31	13	1.21
2	0.27	6	0.43	10	0.58	14	0.64
3	1.20	7	1.19	11	1.40	15	1.37

In order to understand the differences in wear results, particle flows in the simulations are investigated. First the mass flow rate is extracted from the simulations using a mass flow

sensor at the bottom of the chute. The sensor along with the mass flow rates over time are depicted in Figure 7.

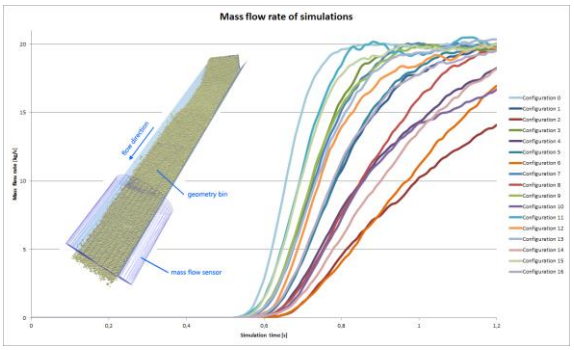

Figure 7: Mass flow rate over time of simulations results (right) and mass flow sensor (left)

As shown in Figure 7, most simulations reach the 20 kg/s. However, some configurations show a slower rise in mass flow rate. Comparing these results with the sliding wear results in Figure 6, a slight correlation exists between the low wear results and the slower flow of material at the end of the chute. The smooth surface chute first reaches 20kg/s, and configuration 2 shows the lowest wear results but the slowest flow rate.

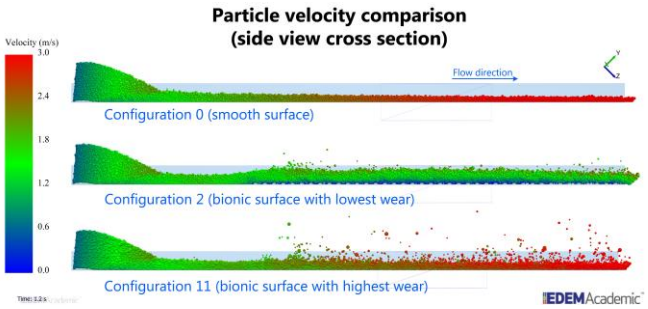

Figure 8: Particle velocity comparison

Particle velocity comparisons for configurations 0, 2 and 11 are shown in Figure 8. Configuration 0 shows a thin layer of particles steadily increasing in speed along the length of the chute. Configuration 11, with small, strongly ellipsoidal convexes and the highest wear results, shares this speed increase along the chute. It can be seen that particles are colliding with the small convexes, causing them to move upwards, away from the chute.

For configuration 2, the velocity of the particles seems to remain steady and a thick layer of particles is shown across the entire chute length. Less particles are flying off the chute in this configuration, compared to configuration 11. The particles in touch with the chute surface seem to be almost at a standstill, while at the top of the particle bed the particles have the highest speed. The lack of particle velocity increase appears to be the explanation of the slower rise in mass flow rate.

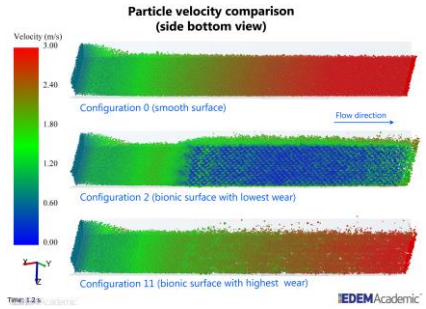

Figure 9: Particle velocity comparison at 1.2 seconds

Figure 9 shows the bottom of the three configurations to see what influence the bionic surface has on the particle flow. At the start of the bionic surface, there is more green visible than in the middle of the bionic surface. This suggests the particles at first are not entirely slowed down by the convexes. At the end of the chute the density of the particle stream is lower than in the middle of the bionic surface, suggesting the flow rate has not reached its full potential of approximately 20 kg/s. When comparing configuration 11 with configuration 0, it is noted that the length of the particles with low velocity (green) is slightly longer. This proves that the particles are slowed down marginally by the bionic surface.

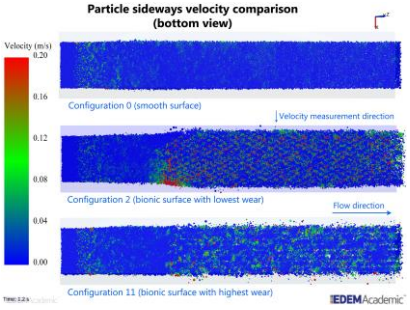

Figure 10: Particle velocity sideways from flow direction comparison at 1.2 seconds

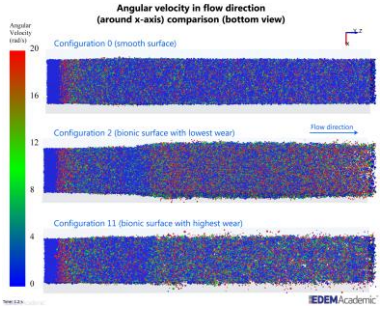

Figure 11: Angular particle velocity comparison at 1.2 seconds (bottom view with transparent chute)

Figure 10 shows the sideways particle velocity (perpendicular to the flow direction). As expected the smooth surface chute does not cause the particles to move sideways much, away from their original trajectory downwards. Configuration 2 shows that the particles at the bottom are moving. The pattern of red particles of configuration 2 in Figure 10 corresponds to the convexes of the bionic surface. This shows that these particles are moving around the convexes by rolling or sliding sideways around them. Configuration 11 in Figure 10 shows that the small convexes cause the smooth, almost strictly downward flow of configuration 0 to be disrupted.

The angular velocity in forward/downwards direction of the particles is analysed in Figure 11. From configuration 0 in Figure 11 there appears to be a relatively even distribution of rolling and (most probably) sliding particles in touch with the surface of the chute, depicted by the mix of red, green and blue particles. The majority of particles are blue, and considering the speed these particles have, it is likely to assume sliding of particles is mainly dominant over the chute's surface.

In configuration 2 it is noted that a lot more particles appear to be rolling. Unlike the sideways and total velocities in Figure 9 and Figure 10, there is no distinct pattern that

matches the convex pattern in this figure. This suggests that the particles are not only rolling around the convexes, but also over them. Configuration 11 shows some improvement in the rise of particles that are rolling, but the change is more significant in configuration 2.

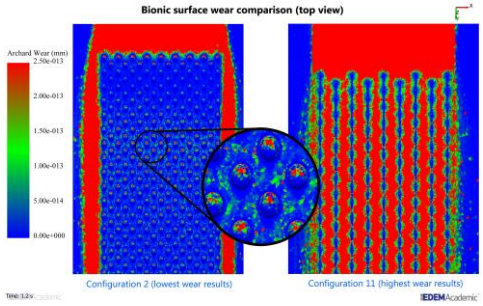

Figure 12: Sliding wear visualization in EDEM with lowest (left) and highest (right) wear gradient

The wear results are visualised in Figure 12. Configuration 2 sees a lot of wear above and on the sides of the bionic surface, but relatively little over the bionic surface. The first two rows of convexes have red tops, which is likely caused by the impact of the particle stream onto the top of these convexes. The next few convex rows suffer very little wear, followed by an area where there is also some wear in the areas in between the convexes. Even lower on the bionic surface the wear pattern seems to become steady, which is the same over the rest of the length of the bionic surface. It appears that the particle stream follows a transition phase from smooth surface to a steady flow over the bionic surface. This is the reason for the position of the wear measurement lower on the chute's surface. The top of the convexes logically experience the most wear, whereas at the bottom of convexes there is virtually no wear, visualised in the circular close-up in Figure 12.

The wear pattern of the bionic surface of configuration 11 shows a high amount of wear. Configuration 11 has relatively small convexes, which are spaced relatively far apart (perpendicular to the flow direction). It appears that the particle flow is not disrupted in these wide spaces between columns of convexes. This uninterrupted sliding of the stream causes similar as wear results in these spaces. The small convexes are effective however in reducing the wear in the areas closely around them, depicted by the blue ellipses in Figure 12 (right).

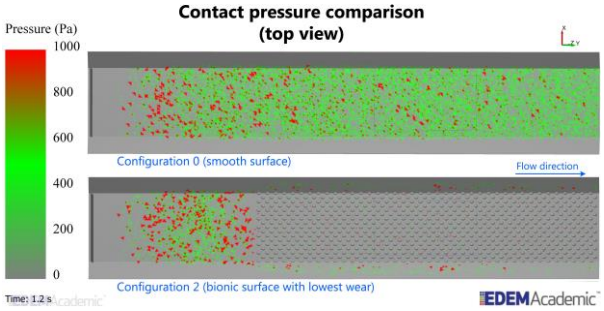

Figure 13: Contact pressure of smooth surface chute and bionic surface chute with lowest wear results

The contact pressures of the chutes of configuration 0 and configuration 2 are depicted in Figure 13. The results vary greatly between the smooth areas and the bionic surface areas. It is noted that the contact pressure is greatly reduced in the area of the bionic surface, despite this area having a much higher stack of particles above it.

3.2 Full factorial design results

The residual plots of the wear gradient from Figure 14 can indicate whether there are abnormalities in the data set like duplicates, but more importantly, they can indicate if a linear or non-linear model is applicable [23, 24]. The normal probability plot shows that the residuals follow a linear line to a satisfactory extend, while the remainder of plots show a random pattern of residuals. This indicates that a linear model is valid for this data set.

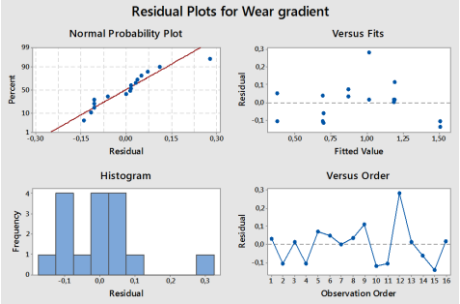

Figure 14: Residual plots of wear gradient

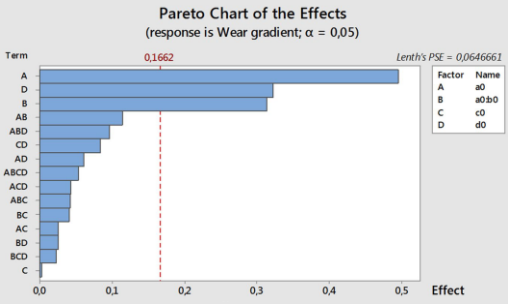

Figure 15: Pareto chart showing factors of influence on sliding wear

To find the factors of influence on the sliding wear a Pareto chart is used chart and the significance of the factors is considered at a confidence level of 95% (α= 0.05) [25]. Figure 15 shows the absolute values of the standardised effects from the largest effect to the smallest effect. The standardised effects are t-statistics that test the null hypothesis that the effect is 0 [25]. The chart also plots a reference line to indicate which effects are statistically significant. Figure 15 clearly shows that the factor a_0 has the biggest effect on sliding wear. The ratio a_0 : b_0 is also a factor of influence, to a similar degree as d_0. The factor c_0, representing the vertical space between convexes, is shown no influence on sliding wear. Also interactions between parameters are shown to be statistically insignificant.

Figure 16 shows the main effects the different factors have on the sliding wear. It can be seen that the higher value of factor a_0 can significantly reduce wear. A low value of a_0:b_0 results in less wear, suggesting that a more circular convex is better in minimising wear. C_0 has no effect on the sliding wear and lowering d_0 can reduce wear.

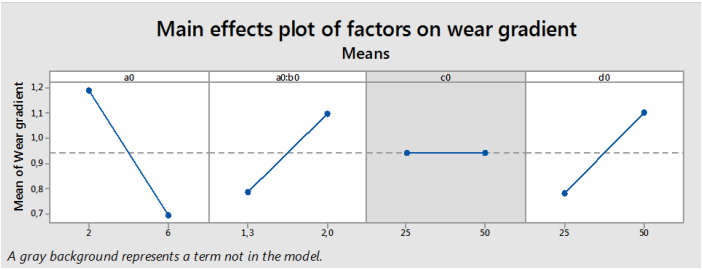

Figure 16: Main effects plot of factors on wear gradient

Figure 17 shows the interactions between the four parameters. It shows that none of the plot lines have a significantly different slope, which proves their interactions are not strong. The biggest difference can be seen in the top left plot showing the interaction between a_0 and a_0:b_0. The slight deviation in line slope suggests that the effect of a_0 slightly depends on the level of a_0:b_0. This effect and all other interactions are insignificant however, as mentioned

earlier and shown in Figure 15.

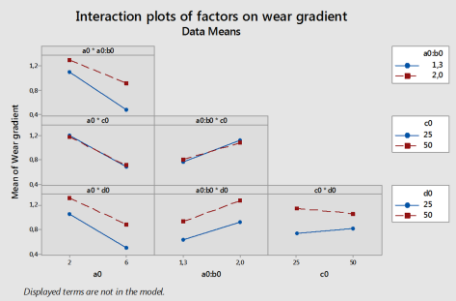

Figure 17: Interactions between parameters

4 DISCUSSION

This part will discuss the results of the DoE and draw preliminary conclusions on the optimisation of the bionic geometry. Also the next step in the optimisation process is explained.

4.1 Full factorial design discussion

Based on the FFD analysis and the analysis of the particle flow in EDEM in subpart 3.1, several conclusions can be drawn on the effects of the bionic geometry parameters on the sliding wear. A clear overview of these conclusions is presented in Table 5. In separate paragraphs below each conclusion is individually discussed.

Table 5: Effects of bionic geometry parameters on sliding wear

Factors	Influence on minimising wear
Vertical convex radius a_0	Higher value has significant influence
Convex eccentricity a_0:b_0	Lower value has influence
Vertical distance c_0	Has no influence
Horizontal distance d_0	Lower value has influence
Interactions between factors	Insignificant influence

Vertical convex radius a_0 Increasing a_0 means that a bigger convex size is better at reducing wear. It can be seen that with large convexes the particle flow gets slowed down and the particles encouraged to slowly roll downwards at the chute's surface. The particles closest to the chute's surface are travelling at very low speeds and are rolling much more due to the bionic surface which reduces wear greatly.

Convex eccentricity a_0:b_0 When the ratio a_0:b_0 is lower, wear reduction is more efficient. This means that the more circular the shape of the convexes, the better they are at slowing down the particle flow and facilitating particles to roll rather than slide.

Vertical distance c_0 The distance between convexes in flow direction, c_0, has no influence on the sliding wear.

Horizontal distance d_0 When the d_0 is too high, it will cause more wear on a bionic surface. The space between columns of convexes will allow particles to slide directly, and no particles can be slowed down.

Interactions between factors From the analysis it can be concluded that there are very

small interactions between the geometric parameters.

5 CONCLUSIONS

Through FFD experiment method, it is concluded that a_0, a_0:d_0 and d_0 have significant influence on wear, while c_0 and interactions have almost no influence on wear. A bionic surface works by slowing down the particle stream near the surface of the chute and force the particles to roll instead of slide. This causes the rest of the particles to roll or slide over a bottom layer of particles and prevents particles from sliding directly over the chute's surface, greatly reducing wear on the chute. The bionic method can be a reference for other bulk handling equipment surfaces suffering mechanical wear caused by particulate solids.

However, it is possible that a different PSD can provide different results. So, experiments would be the best methodology to validate the finding of this research. The circular shape of iron ore particles make it ideally shaped to induce the rolling of particles by the bionic surface. Angular particles could behave very differently over a bionic surface and should be further investigated.

REFERENCES

[1] Wei Chen, Subhankar Biswas, Alan Roberts, Jayne O'Shea, Kenneth Williams. Abrasion wear resistance of wall lining materials in bins and chutes during iron ore mining. *International Journal of Mineral Processing*, 167(2017)42-48.

[2] G. Chen and D. Schott, Surface Wear Reduction of Bulk Solids Handling Equipment Using Bionic Design, Ph.D. thesis, TU Delft (2017).

[3] Alan W Roberts. Chute performance and design for rapid flow conditions. *Chemical engineering & technology*, 26(2):163–170, 2003.

[4] A. Chumber. Handling aggressive goods: Using wear resistant linings to ensure material flow and reduce abrasion. *Bulk Solids Handling*, 33(2):32–33, 2013. cited By 0.

[5] P. Hilgraf. Basic principles of wear protection technology for bulk materials (part 1) [grundlagen der verschleischutz-technik fr schttg ter (teil 1)]. *ZKG International*, 62(10):53–63, 2009.

[6] P. Hilgraf. Basic principles of wear protection technology for bulk materials (part 2) [grundlagen der verschlei-bschutztechnik fr schttgter (teil 2)]. *ZKG International*, 62(11):56–72, 2009.

[7] Dietmar Schulze. *Powders and bulk solids: behavior, characterization, storage and flow*. Springer Science & Business Media, 2007.

[8] Peter A Cundall and Otto DL Strack. A discrete numerical model for granular assemblies. *Geotechnique*, 29(1):47–65, 1979.

[9] EDEM Team. *EDEM 2.6 Theory Reference Guide*. DEM Solutions, 2015.

[10] Paul W Cleary. Predicting charge motion, power draw, segregation and wear in ball mills using discrete element methods. *Minerals Engineering*, 11(11):1061–1080, 1998.

[11] Andrew P Grima and Peter W Wypych. Investigation into calibration of discrete element model parameters for scale-up and validation of particle–structure interactions under

impact conditions. *Powder Technology*, 212(1):198–209, 2011.

[12] Kevin Francis Malone and Bao Hua Xu. Determination of contact parameters for discrete element method simulations of granular systems. *Particuology*, 6(6):521–528, 2008.

[13] Paul W Cleary, Phil Owen, David I Hoyer, and Steve Marshall. Prediction of mill liner shape evolution and changing operational performance during the liner life cycle: Case study of a hicom mill. *International journal for numerical methods in engineering*, 81(9):1157–1179, 2010.

[14] Johnny T Kalala and Michael H Moys. Discrete element method modelling of liner wear in dry ball milling. *Journal of the South African Institute of Mining and Metallurgy*, 104(10):597–602, 2004.

[15] Paul W Cleary, Matthew D Sinnott, and Rob D Morrison. Separation performance of double deck banana screens–part 2: Quantitative predictions. *Minerals Engineering*, 22(14):1230–1244, 2009.

[16] Andrew P Grima and Peter W Wypych. Investigation into calibration of discrete element model parameters for scale-up and validation of particle–structure interactions under impact conditions. *Powder Technology*, 212(1):198–209, 2011.

[17] Liyu Xie, Wenqi Zhong, Hao Zhang, Aibing Yu, Yujun Qian, and Yougong Situ.Wear process during granular flow transportation in conveyor transfer. *Powder Technology*, 288:65–75, 2016.

[18] Hao Zhang, Yuanqiang Tan, Dongmin Yang, Francesc Xavier Trias, Shengqiang Jiang, Yong Sheng, and Assensi Oliva. Numerical investigation of the location of maximum erosive wear damage in elbow: Effect of slurry velocity, bend orientation and angle of elbow. *Powder Technology*, 217:467– 476, 2012.

[19] DEM Solutions. EDEM 2.6 User Guide. DEM Solutions, 2015.

[20] Forsström, D. and P. Jonsén (2016). "Calibration and validation of a large scale abrasive wear model by coupling DEM-FEM." Engineering Failure Analysis 66: 274-283.

[21] J. Antony, *Design of Experiments for Engineers and Scientists*, 2nd ed. (Elsevier, Netherlands, 2014).

[22] E. van Enter, *Design of experiments in the transportation domain*, Tech. Rep. (TU Delft, 2017).

[23] R. Kouiden, Residual Plots Revelations, available at http://blog.minitab.com/blog/

statistics-for-lean-six-sigma/residual-revelations, (2017).

[24] *Residual Analysis in Regression*, available at http://stattrek.com/regression/ residual-analysis.aspx?Tutorial=AP, Star Trek Statistics, (2017).

[25] *Effects plots for Analyze Factorial Design*, available at https://support.minitab.com/ en-us/minitab/18/help-and-how-to/modeling-statistics/doe/how-to/factorial/ analyze-factorial-design/interpret-the-results/all-statistics-and-graphs/ effects-plots/,Minitab® support 18, (2017).